

Parameters affecting the seismic response of buildings under bi-directional excitation

Ioanna - Kleoniki M. Fontara^{*}, Konstantinos G. Kostinakis^a, Grigorios E. Manoukas^a
and Asimina M. Athanatopoulou^b

*Department of Civil Engineering, Aristotle University of Thessaloniki, University Campus,
54124, Thessaloniki, Greece*

(Received August 12, 2013, Revised November 17, 2014, Accepted November 18, 2014)

Abstract. The present paper investigates the influence of the orientation of the ground-motion reference axes, the seismic incident angle and the seismic intensity level on the inelastic response of asymmetric reinforced concrete buildings. A single storey asymmetric building is analyzed by nonlinear dynamic analyses under twenty bi-directional ground motions. The analyses are performed for many angles of incidence and four seismic intensity levels. Moreover three different pairs of the horizontal accelerograms corresponding to the input seismic motion are considered: a) the recorded accelerograms, b) the corresponding uncorrelated accelerograms, and c) the completely correlated accelerograms. The nonlinear response is evaluated by the overall structural damage index. The results of this study demonstrate that the inelastic seismic response depends on the orientation of the ground-motion reference axes, since the three individual pairs of accelerograms corresponding to the same ground motion (recorded, uncorrelated and completely correlated) can cause different structural damage level for the same incident angle. Furthermore, the use of the recorded accelerograms as seismic input does not always lead to the critical case of study. It is also shown that there is not a particular seismic incident angle or range of angles that leads to the maximum values of damage index regardless of the seismic intensity level or the ground-motion reference axes.

Keywords: bi-directional excitation; ground-motion reference axes; seismic incident angle; inelastic response; intensity level; damage index; asymmetric single-story building

1. Introduction

For the design of new or the evaluation of existing structures some seismic codes (e.g., EC8, 2003) allow alternatively the use of nonlinear dynamic analysis. In this approach a nonlinear model of the 3D structure is analyzed under a set of pairs of real or artificial accelerograms. This type of analysis introduces some uncertainties concerning the orientation along which the horizontal components of ground motion were recorded (the orientation of ground-motion reference axes), the orientation of seismic incident angle and the record scaling.

In most strong-motion databases the horizontal components of ground motion are given in

^{*}Corresponding author, Ph.D. Student, E-mail: fontara@gpi.uni-kiel.de

^aPh.D.

^bProfessor

respect to the axes they were recorded along. The orientation of the recorded accelerograms is predetermined by the orientation of the recording instrument, which in most cases is arbitrary with respect to the structural axes or the fault on which the earthquake event occurred (Beyer and Bommer 2007). An exception to the latter is the new issue of the NGA database (“Next Generation of Attenuation”), (PEER 2005) in which the components of the records are given in the fault-normal and fault-parallel orientation. Another way of expressing the ground-motion reference axes and the corresponding horizontal accelerograms is along the principal axes of ground motion. If ground motion is considered as a random process the principal axes can be determined as the set of axes along which the covariance between the accelerograms disappears (Penzien and Watabe 1975). In this case the accelerograms are considered as uncorrelated. Despite the fact that the values of acceleration ordinates depend on the reference axes of ground motion, most seismic codes do not give guidance concerning the orientation of the ground-motion horizontal axes. ASCE 41-06 is an exception as it proposes the use of uncorrelated pairs of ground motions (Chen 1975) when time history analysis is performed due to tri- or bi-directional excitation.

In Performance-Based Design, the structural response is estimated for various intensity levels of seismic motion. Hence, recorded ground motions are scaled in order to create records corresponding to the intensity level of interest. The scaling of recorded accelerograms is performed so that the response spectrum produced by the scaled records fits the design spectrum either at a single period or over a period range. Guidelines regarding the records scaling procedure are different among the seismic codes. Therefore, the ordinates of the scaled accelerograms produced by different seismic codes vary significantly (Oyarzo-Vera and Chouw 2008). As a consequence, the structural response produced by accelerograms scaled with different scaling procedures is different. The influence of ground motion scaling on the inelastic response of structures based on scaling techniques different from those given in seismic codes has also been investigated by many researchers (Hancock and Bommer 2008, Catalan *et al.* 2010, Takewaki and Tsujimoto 2011, Wood and Hutchinson 2012, Reyes and Chopra 2012)

The response of the structural system depends on the orientation of the seismic input with regard to structural axes. Rotating the axes along which the horizontal accelerograms are applied leads to different structural response. Several researchers have investigated the influence of seismic incident angle on elastic as well as inelastic structural response. Considering the elastic structural response, analytical formulae for the determination of the critical angle of seismic incidence and the corresponding maximum structural response subjected to three correlated components have been developed (Athanatopoulou 2005). The application of these formulae to symmetric and asymmetric multistory buildings has proved that the maximum value of a response quantity can be up to 180% larger than the response produced when the seismic components act along the structural axes (Athanatopoulou 2005, Athanatopoulou and Avramidis 2006, Athanatopoulou *et al.* 2005, Athanatopoulou *et al.* 2006). Kostinakis *et al.* (2008) examined the critical seismic incident angle and the corresponding maximum response on the basis of the above formulae (Athanatopoulou 2005) for special classes of buildings subjected to isotropic bi-directional ground motion. The results revealed that even in symmetric buildings under isotropic excitation, the maximum response does not occur for seismic components along the structural axes. Also, they proved that the maximum value of the resultant floor displacement as well as the maxima of the resultant frame forces do not depend on the seismic incident angle only in case of symmetric buildings with equal horizontal stiffness along two horizontal orthogonal axes.

Considering the inelastic structural response, MacRae and Mattheis (2000) investigated the influence of angle of incidence on the inelastic behavior of a three-story steel frame building due

to near-fault ground motions. Khoshnoudian and Poursha (2004) evaluated the elastic and inelastic response of a five-story steel building under arbitrary angle of excitation and indicated that the critical angle in non-linear behavior differs from the corresponding critical angle in linear behavior. Rigato and Medina (2007) studied the response of asymmetric and symmetric structures with varying degrees of inelasticity and various fundamental periods of vibration with regard to the angle of incidence by using 39 pairs of ground motion records. They computed the ductility ratios, slab rotations and drift ratios. Results from this study demonstrate that the critical angle for a given response quantity varies with fundamental period, model type and level of inelastic behavior and it is difficult to be determined a priori as in case of elastic structures. Lagaros (2010a, b) investigated the influence of the incident angle on the results of multicomponent incremental dynamic analysis (MIDA). He analyzed a symmetric and an asymmetric three-storey 3D r/c building. The outcome of the study enforced the need to take into account the randomness of both record and incident angle. For this reason, a new procedure for performing MIDA has been introduced with variable pairs of record-incident angle that are generated using the Latin hypercube sampling (LHS). The proposed methodology was incorporated into the life cycle cost analysis procedure in order to assess two reinforced concrete buildings having symmetrical and irregular plan views (Lagaros 2010b). Furthermore, Lucchini *et al.* (2011) showed that the torsional response of a two-way asymmetric single-story building under biaxial excitation is affected by the angle of incidence. Zhang *et al.* (2011, 2012) demonstrated that seismic incident angle affects the elastic as well as inelastic response of symmetric buildings. Another study carried out by Nguyen and Kim (2013) investigated the influence of seismic incident angles on single storey asymmetric buildings. However, none of the above mentioned studies evaluated the structural response taking into account the influence of the orientation of ground-motion reference axes.

The present study examines the influence of seismic incident angle on the damage index of an asymmetric single storey r/c building subjected to the recorded, the uncorrelated and completely correlated pairs of accelerograms (orientation of ground-motion reference axes). Moreover, the influence of seismic intensity level on inelastic structural response over all seismic incident angles is investigated. For this purpose, nonlinear time history analyses under twenty bi-directional ground motions are conducted. The analyses are performed for many angles of seismic incidence and four different seismic intensity levels.

2. Description of the structure

The single storey reinforced concrete asymmetric building shown in Fig. 1 with fundamental period $T=0.3s$ is used in the present study. The design of the building is performed using the Greek Code for the Design and Construction of Concrete Works on the basis of response values produced by gravity and seismic loads. The seismic analysis is conducted by the response spectrum method using the elastic spectrum suggested by the Greek Seismic Code (EAK) for seismic zone III (0.36 g) and site class B, which corresponds to site class D according to FEMA.

It is common research practice to perform the comparison and evaluation of various analysis parameters or design methods - in a first step - on the basis of a quite simple example. Also, for initial study of the ground-motion reference axes, the author's aim is to use a simple stiff structure (period elongation in the inelastic range is expected) under an adequate number of ground motion records with various ground motion characteristics. Such simple structures are widely used by

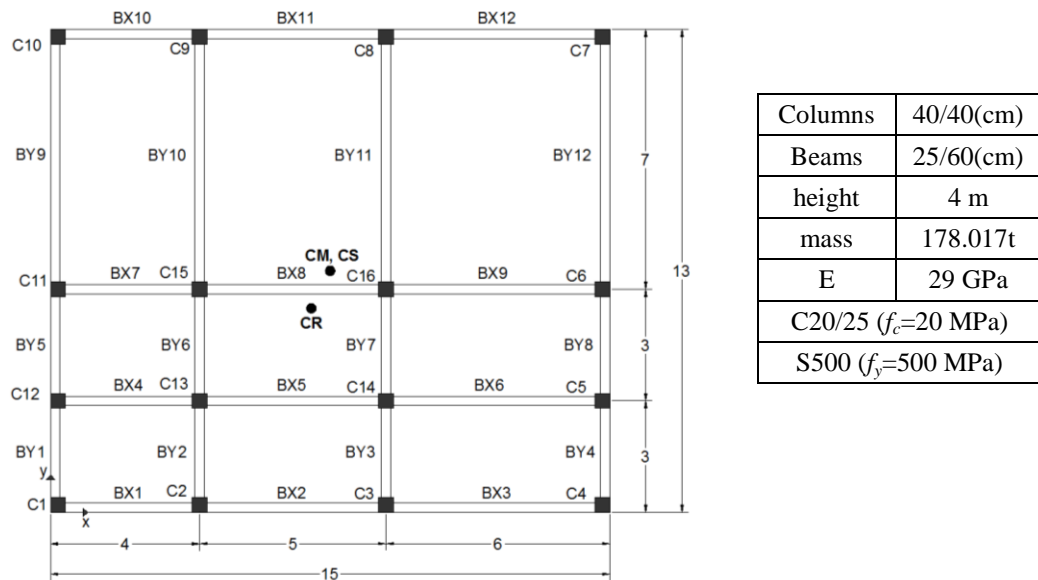


Fig. 1 Plan view and geometrical properties of the single storey asymmetric building (CM: Mass Center, CR: Center of Rigidity, CS: Center of Strength)

many researchers (Beyer and Bommer 2007, MacRae and Mattheis 2000, Stathopoulos and Anagnostopoulos 2005, Dolsek and Fajfar 2002) as a first step, for evaluation of various analysis parameters.

3. Ground motions

3.1 Records selection

A suite of 20 pairs of horizontal ground motion records (Table 1) are obtained from the PEER strong motion database according to magnitude, closest distance to fault rupture and site class. In particular, ground motions are selected to fall into the following bins: $M_s=[5.7, 7.3]$, $R_{rup}=[6, 57.4]$ (M_s : seismic magnitude, R_{rup} (km): closest distance to fault rupture) and recorded on site class *D* in accordance to FEMA classification.

3.2 Ground-motion reference axes

As previously mentioned, any rotation of the horizontal components of the record modifies the values of the acceleration ordinates. For this purpose, in order to examine the influence of the orientation of the ground-motion reference axes, the present paper takes into consideration discrete cases of ground motion components: the correlated recorded accelerograms, the corresponding uncorrelated accelerograms and the completely correlated accelerograms.

The horizontal accelerograms of a record possess, in general, a random degree of correlation. However, there is a specific set of axes for which the covariance disappears. This set of axes,

Table 1 Data of the records considered in this study

No	Ground motion	Date	Station	M ¹ (Ms)	R ² (Km)	C ³ (deg)
1	Northridge	17/1/1994	24303 L.A., Hollywood Storage Bldg.	6.7	25.5	360 90
2	Northridge	17/1/1994	24538 Santa Monica CityHall	6.7	27.6	360 90
3	Loma Prieta	18/10/1989	47381 Gilroy#3, Sewage Treatment Plant	7.1	14.4	0 90
4	Loma Prieta	18/10/1989	58393 Hayward,John Muir School	7.1	57.4	0 90
5	Whittier Narrows	10/1/1987	14368 Downey,Country Maintennance	5.7	18.3	180 270
6	Imperial Valley	15/10/1979	5059 El Centro #13, Strobel Residence	6.9	21.9	140 230
7	San Fernando	9/2/1971	135 L. A., Hollywood Storage Bldg.	6.6	21.2	90 180
8	Loma Prieta	18/10/1989	1652 USGS, Aderson Dam (Downstream)	6.9	21.4	270 360
9	Northridge	17/1/1994	24087 CDMG Arleta-Nordhoff FireStation	6.7	9.2	360 90
10	Landers	18/10/1989	23 SCE Coolwater	7.3	21.2	LN TR
11	Landers	18/10/1989	12149 CDMG Desert Hot Springs	7.3	23.2	0 90
12	Imperial Valley	10/1/1987	6618 UNAM/UCSD Agrarias	6.5	12.9	273 3
13	Imperial Valley	15/10/1979	5055 USGS Hotville PostOffice	6.5	7.5	225 315
14	Loma Prieta	9/2/1971	47524 CDMG Hollister - South And Pine	6.9	28.8	0 90
15	Imperial Valley	17/1/1994	117 USGS El Centro Array #9	7	8.3	180 270
16	Landers	17/1/1994	5070 USGS North Palm Springs	7.3	24.2	0 90
17	N Palm Springs	18/10/1989	12025 CDMG Palm Springs Airport	6	16.6	0 90
18	Northridge	18/10/1989	90006 USC Sun Valley-RoscoeBlvd	6.7	12.3	0 90
19	Landers	10/1/1987	22074 CDMG Yermo Fire Station	7.3	24.9	270 360
20	Coyote Lake	15/10/1979	47381 CDMG Gilroy Array #3	5.7	6	50 140

¹Magnitude²Closest distance to fault rupture³Component

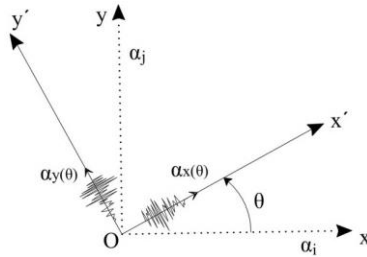


Fig. 2 Accelerograms along the rotated axes x' and y'

which was firstly introduced by Arias (1970), defines the principal axes of the seismic motion along which the accelerograms are considered as uncorrelated. The principal axes are produced by rotating the horizontal components of the record in the original orientation counterclockwise by an angle θ_{cr} (Eq. (1)). The acceleration histories are rotated by an angle θ using Eq. (2)

$$\tan 2\theta_{cr} = \frac{2 \cdot \sigma_{ij}}{\sigma_{ii} - \sigma_{jj}}, \quad \sigma_{ij} = \frac{1}{s} \int_0^s \alpha_i(t) \cdot \alpha_j(t) dt \quad (1)$$

$$\begin{pmatrix} \alpha_{x(\theta)}(t) \\ \alpha_{y(\theta)}(t) \end{pmatrix} = \begin{bmatrix} \cos\theta & \sin\theta \\ -\sin\theta & \cos\theta \end{bmatrix} \cdot \begin{pmatrix} \alpha_i(t) \\ \alpha_j(t) \end{pmatrix} \quad (2)$$

where $\alpha_i(t)$ and $\alpha_j(t)$ are the components in the original orientation, s the total duration of the ground motion and $\alpha_{x(\theta)}(t)$ and $\alpha_{y(\theta)}(t)$ are the rotated components by an angle θ (Fig. 2). So, by a simple matrix multiplication of the two time histories, the uncorrelated components of the record are computed. In practice, according to the Penzien and Watabe (1975) model, it is demonstrated that the major principal axis is directed towards the epicenter. The major principal direction is defined with regard to the original orientation by the angle θ_{cr} (Eq. (1)) (Fig. 3(b)).

Furthermore, when the correlation coefficient of the horizontal components of the ground motion attains its maximum value, the accelerograms are completely correlated. Completely correlated accelerograms of a ground motion are determined by rotating the uncorrelated horizontal components of the record counterclockwise by an angle $\theta=45^\circ$ (Fig. 3(c)). Hence, substituting $\theta=\theta_{cr}+45^\circ$ and $\alpha_i(t)$ and $\alpha_j(t)$ with the uncorrelated components in Eq. (2), gives the completely correlated components.

In Fig. 4 the SRSS spectra of the two horizontal components of the selected ground motions for the recorded, uncorrelated and completely correlated pairs of accelerograms are depicted. We can see that the SRSS spectra of the recorded, the uncorrelated and the completely correlated pairs of accelerograms corresponding to the same ground motion are different.

3.3 Records scaling

The pairs of recorded, uncorrelated and completely correlated accelerograms are scaled according to two different procedures prescribed in ASCE 41-06 and EC8-Part 1 so as to match the design spectrum suggested by the Greek Seismic Code. According to ASCE 41-06, in the case of the closest distance to fault rupture being greater than 5km, it is stated that the average SRSS spectrum of the two components of all records should be scaled not to fall below 1.4 times the

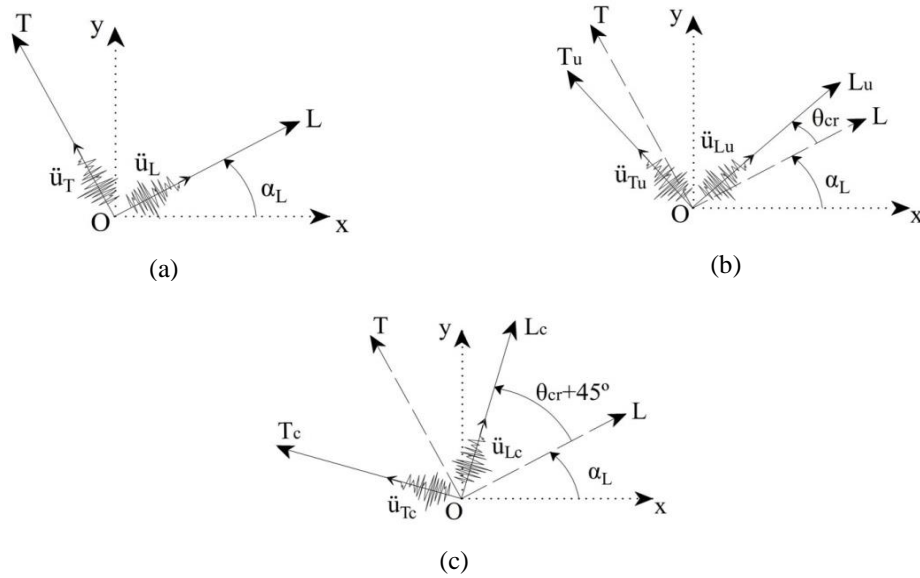


Fig. 3 (a) Recorded accelerograms along L and T axes; (b) Uncorrelated accelerograms along Lu and Tu axes; (c) Completely correlated accelerograms along L_c and T_c axes

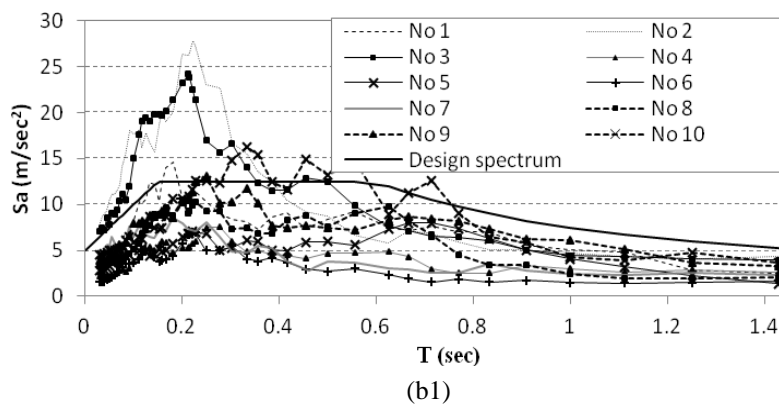
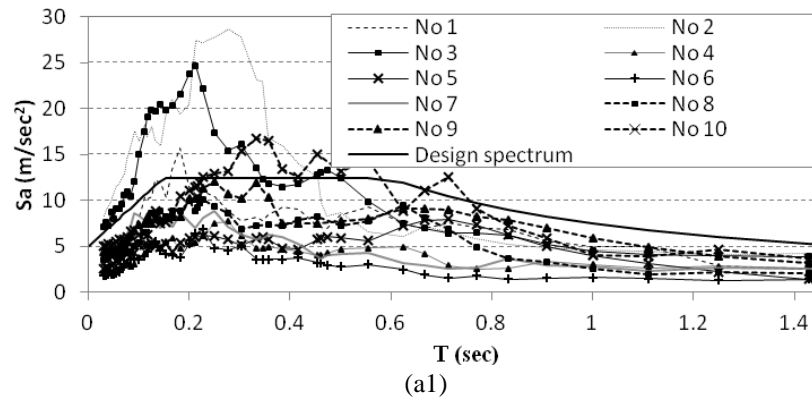
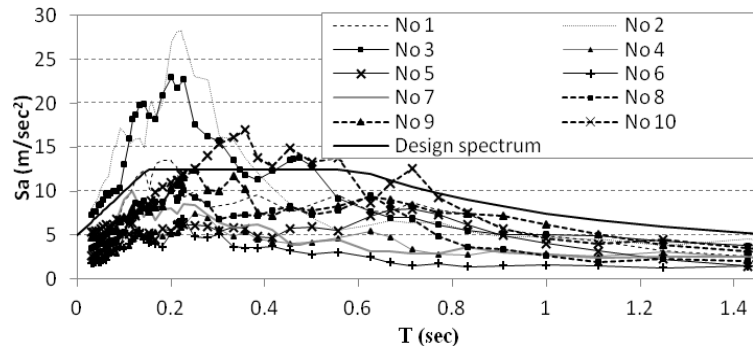
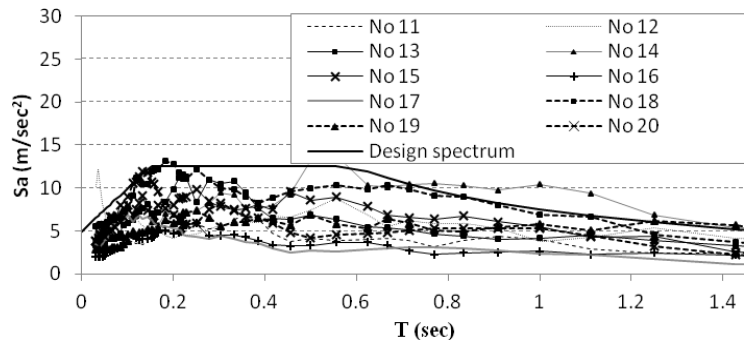


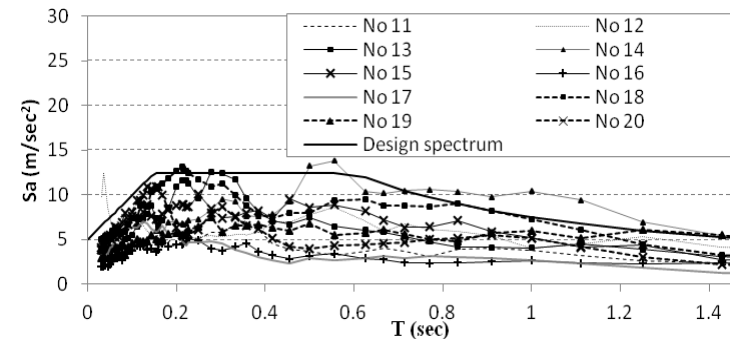
Fig. 4 The SRSS spectra of the two horizontal components; (a1,2) recorded accelerograms, (b1,2) uncorrelated accelerograms and (c1,2) completely correlated accelerograms



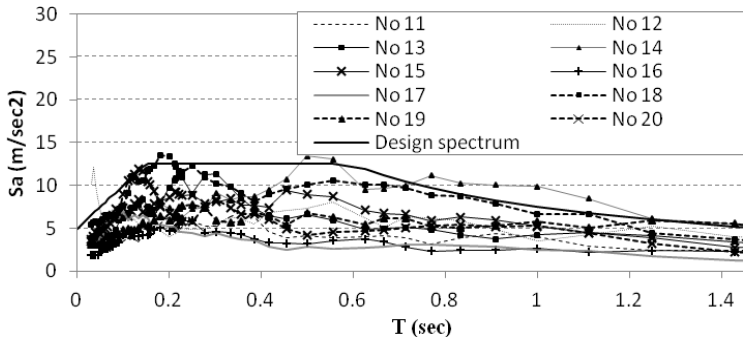
(c1)



(a2)



(b2)



(c2)

Fig. 4 Continued

design spectrum of a single component (a single scale factor is determined for each pair of records). The period range over which matching of design spectrum and average spectrum of the records is required, is $0.2T_1-1.5T_1$, where T_1 is the fundamental period of the structure. In EC8-Part1 the scaling procedure is based on the mean spectrum of all horizontal components of the records, considered as individual ground motions. Also, EC8-Part1 states one more rule concerning the record scaling, supplementary to one previously mentioned. According to this rule the accelerograms should be scaled to match the peak ground acceleration. It is also noted that, according to EC8-Part1, the scaling procedure is conducted over the period range $0.2T_1-2.0T_1$, where T_1 is the fundamental period of the structure along the direction in which the seismic excitation will be applied.

In Table 2 the scale factors for the recorded, the uncorrelated and the completely correlated accelerograms are presented. As can be seen, the scale factors corresponding to the recorded, the uncorrelated and the completely correlated components of the same excitation are different for both ASCE 41-06 and EC8-Part 1 scaling procedures. Note that the scale factor for the uncorrelated components of San Fernando ground motion obtained by EC8 procedure is 1.80 and 2.4 times larger than the scale factors determined for the recorded and the completely correlated components respectively. Also, it is observed that EC8-Part 1 scaling procedure provides larger scale factors than the ones produced by ASCE 41-06 for the ground motions used in the present study. For the Whittier Narrows and the San Fernando ground motions and for the uncorrelated accelerograms the scale factor provided by EC8-Part 1 is up to 2.2 times larger than the corresponding one computed by the ASCE 41-06 scaling procedure.

Table 2 Scale factors produced by the recorded, the uncorrelated and the completely correlated accelerograms

No	Ground motion	Accelerograms	S.F.NEHRP	S.F.EC8
1	Northridge	Recorded	1.56	2.13
		Uncorrelated	1.57	2.25
		Completely correlated	1.54	2.58
2	Northridge	Recorded	1.38	2.00
		Uncorrelated	1.25	2.04
		Completely correlated	1.35	2.06
3	Loma Prieta	Recorded	1.00	1.92
		Uncorrelated	1.00	1.99
		Completely correlated	1.01	1.72
4	Loma Prieta	Recorded	2.96	4.56
		Uncorrelated	3.08	4.10
		Completely correlated	2.92	3.31
5	Whittier Narrows	Recorded	2.60	3.65
		Uncorrelated	2.46	5.49
		Completely correlated	2.58	3.04
6	Imperial Valley	Recorded	3.58	6.78
		Uncorrelated	3.91	5.84
		Completely correlated	3.54	6.31
7	San Fernando	Recorded	2.88	4.72
		Uncorrelated	3.88	8.50
		Completely correlated	2.84	3.55

Table 2 Continued

8	Loma Prieta	Recorded	1.94	1.96
		Uncorrelated	2.06	2.22
		Completely correlated	1.94	1.97
9	Northridge	Recorded	1.54	1.81
		Uncorrelated	1.63	2.07
		Completely correlated	1.60	1.65
10	Landers	Recorded	1.59	1.90
		Uncorrelated	1.60	1.74
		Completely correlated	1.57	1.70
11	Landers	Recorded	3.33	3.90
		Uncorrelated	2.98	4.35
		Completely correlated	3.34	3.76
12	Imperial Valley	Recorded	2.81	3.50
		Uncorrelated	2.67	3.98
		Completely correlated	2.82	2.87
13	Imperial Valley	Recorded	1.90	2.51
		Uncorrelated	1.91	2.57
		Completely correlated	2.04	2.55
14	Loma Prieta	Recorded	2.22	2.91
		Uncorrelated	2.23	2.98
		Completely correlated	2.12	2.52
15	Imperial Valley	Recorded	1.69	2.44
		Uncorrelated	1.59	2.24
		Completely correlated	1.67	1.98
16	Landers	Recorded	3.53	4.14
		Uncorrelated	4.08	4.42
		Completely correlated	3.55	4.08
17	N Palm Springs	Recorded	4.72	5.04
		Uncorrelated	4.97	6.23
		Completely correlated	4.56	5.02
18	Northridge	Recorded	1.38	1.52
		Uncorrelated	1.56	1.72
		Completely correlated	1.40	1.53
19	Landers	Recorded	2.74	3.29
		Uncorrelated	2.59	3.04
		Completely correlated	2.48	2.71
20	Coyote Lake	Recorded	2.36	3.32
		Uncorrelated	2.70	3.87
		Completely correlated	2.35	3.54

4. Nonlinear dynamic analysis

Nonlinear dynamic analyses have been carried out for twenty bi-directional ground motions (Table 1) represented by the aforementioned pairs of accelerograms (recorded, uncorrelated and completely correlated). In order to examine the influence of seismic incident angle, the two

horizontal accelerograms are applied along horizontal orthogonal axes forming with the structural axes an angle $\theta=0^\circ, 10^\circ, 20^\circ, \dots, \dots, 350^\circ$. The nonlinear analyses are performed by the aid of computer program Ruaumoko 3D (Carr 2004).

For the evaluation of the inelastic structural behavior damage indices have been used. In general, damage indices estimate quantitatively the degree of seismic damage that a cross-section as well as a whole structure has suffered. A damage index is a quantity with zero value when no damage occurs and a value of 1 when failure or collapse occurs. However, the damage index referring to the whole structure may exceed the value of 1 (Park and Ang 1985).

In the present paper, the modified Park and Ang (1985) damage index, given by Eq. (3), has been used

$$DI = \frac{\phi_m - \phi_y}{\phi_u - \phi_y} + \frac{\beta}{M_y \cdot \phi_u} \cdot E_T \tag{3}$$

where DI is the local damage index, ϕ_m the maximum curvature attained during the load history, ϕ_u the ultimate curvature capacity of the section, ϕ_y the yield curvature, β a strength degrading parameter, M_y the yield moment of the section and E_T the dissipated hysteric energy. Eq. (3) calculates the local damage index (cross-section damage). This research addresses the overall structural damage index (OSDI) computed as the mean value of all local damage indices weighted by the local energy absorptions (Eq. (4)).

$$OSDI = \frac{\sum_{i=1}^n [D.I.col.weighted.,i \cdot (E_{x,col,i} + E_{y,col,i})] + \sum_{i=1}^m [D.I.beam,i \cdot E_{beam,i}]}{\sum_{i=1}^n [(E_{x,col,i} + E_{y,col,i})] + \sum_{i=1}^m [E_{beam,i}]} \tag{4}$$

where $D.I.col.weighted.,i$ is the energy weighted average of the column damage indices due to both horizontal components of an excitation, $D.I.beam,i$ the beam damage index, E the dissipated energy and n, m the number of columns and beams respectively. Since the locations having high damage indices will also be the ones which absorb large amounts of energy, the weighted damage index puts a higher weighting on the more heavily damaged members. Thus, to a first approximation, the weighted damage index reflects the state of the most heavily damaged members.

Nonlinear dynamic analyses under the twenty bi-directional ground motions shown in Table 1 are conducted for four different seismic intensity levels: a) seismic intensity that causes minor damage, b) seismic intensity that causes moderate damage, c) seismic intensity that causes severe damage and d) real seismic intensity. To accomplish this, the three pairs of accelerograms (the scaled ones so as to match the design spectrum) are multiplied by an appropriate factor $sf_{intensity\ level}$. That is, the final scale factor SF is the product of two factors: i) the factor $sf_{scaling}$ produced by the scaling procedure and ii) the factor $sf_{intensity\ level}$ used to achieve the appropriate intensity level ($SF=sf_{scaling} \times sf_{intensity\ level}$). The first three classifications (a, b and c) correspond to values of the maximum overall damage index over all seismic incident angles (denoted for brevity in the following as $M_{max}OSDIA$) ranging from 0 to 0.25, from 0.25 to 0.70 and from 0.70 to 1.00, respectively. The last classification (real seismic intensity) corresponds to the value of $M_{max}OSDIA$ when the input pairs of accelerograms are multiplied only with the scale factor produced by the scaling procedure ($SF=1 \times sf_{scaling}$).

The nonlinear dynamic analyses are performed for accelerograms scaled according to ASCE 41-06 procedure. The present paper takes into consideration two variants of the scale factors produced by the scaling procedure ($sf_{scaling}$) for each pair of accelerograms. Firstly, the recorded,

the uncorrelated as well as the completely correlated accelerograms are multiplied with the same scale factor. That is the biggest among the ones computed by the scaling procedure for the three individual pairs corresponding to the same ground motion (Table 3). Secondly, each individual pair of accelerograms is multiplied by the scale factor determined by the scaling procedure, which (scale factor) is different for each individual pair of accelerograms corresponding to the same seismic motion for the majority of the ground motions used (Table 4). Note that the appropriate factors used to get the four different intensity levels ($sf_{\text{intensity level}}$) are the same in both the aforementioned variants (Tables 3 and 4). The present study required a total of 17280 nonlinear analyses runs (20×3 pairs of accelerograms \times 36 incident angles \times 4 seismic intensity levels \times 2 scale factors).

Table 3 M_{max} OSDIA for four seismic intensity levels. The individual pairs of accelerograms are scaled by the same factor

No	Ground motion	$\frac{sf_{\text{scaling}}^2}{sf_{\text{intensity level}}^3} =$	SF	Accelerograms						
				Recorded		Uncorrelated		Completely correlated		
				Angle (deg)	D ¹	Angle (deg)	D ¹	Angle (deg)	D ¹	
1	Northridge	[a] ⁴	1.57×0.42=	0.66	60	0.08	210	0.07	260	0.08
		[b] ⁵	1.57×0.55=	0.86	250	0.63	230	0.70	110	0.63
		[c] ⁶	1.57×0.70=	1.10	250	0.82	70	0.95	260	0.89
		[d] ⁷	1.57×1.00=	1.57	270	1.14	50	1.06	120	1.05
2	Northridge	[a]	1.38×0.20=	0.28	160	0.05	260	0.06	310	0.05
		[b]	1.38×0.30=	0.41	140	0.59	240	0.67	290	0.59
		[c]	1.38×0.50=	0.69	230	1.00	0	1.00	110	0.92
		[d]	1.38×1.00=	1.38	200	1.17	260	1.16	320	1.17
3	Loma Prieta	[a]	1.01×0.40=	0.40	330	0.16	330	0.15	20	0.16
		[b]	1.01×1.00=	1.01	330	0.68	160	0.67	20	0.68
		[c]	1.01×1.40=	1.41	60	0.87	80	0.87	30	0.86
		[d]	1.01×1.00=	1.01	330	0.77	160	0.67	20	0.68
4	Loma Prieta	[a]	3.08×0.30=	0.92	260	0.14	70	0.13	120	0.14
		[b]	3.08×0.70=	2.16	90	0.65	90	0.64	120	0.65
		[c]	3.08×1.00=	3.08	270	0.88	90	0.88	320	0.90
		[d]	3.08×1.00=	3.08	270	0.88	90	0.88	320	0.90
5	Whittier Narrows	[a]	2.60×0.40=	1.04	260	0.13	280,290	0.13	330	0.13
		[b]	2.60×0.90=	2.34	80	0.70	100	0.67	150	0.70
		[c]	2.60×1.10=	2.86	240	0.80	280	0.82	330	0.79
		[d]	2.60×1.00=	2.60	250	0.75	270	0.76	140	0.77
6	Imperial Valley	[a]	3.91×0.30=	1.17	200	0.22	240	0.22	280,290	0.22
		[b]	3.91×0.60=	2.35	20	0.68	70	0.68	110	0.68
		[c]	3.91×0.85=	3.32	210	0.85	240	0.87	300	0.85
		[d]	3.91×1.00=	3.91	20	0.99	250	1.05	300	1.00
7	San Fernando	[a]	3.88×0.30=	1.16	260	0.24	280	0.25	330	0.24
		[b]	3.88×0.50=	1.94	270	0.61	290	0.59	310	0.61
		[c]	3.88×0.70=	2.72	90	0.82	290	0.79	130	0.84
		[d]	3.88×1.00=	3.88	80	1.13	80	1.20	120	1.18

Table 3 Continued

8	Loma Prieta	[a]	2.06×0.50=	1.03	50	0.21	180,190	0.20	230	0.21
		[b]	2.06×0.70=	1.44	50	0.43	190	0.43	230	0.43
		[c]	2.06×1.00=	2.06	230	0.79	350	0.77	230	0.75
		[d]	2.06×1.00=	2.06	230	0.79	350	0.77	230	0.75
9	Northridge	[a]	1.63×0.30=	0.49	140	0.11	260	0.11	120	0.10
		[b]	1.63×0.35=	0.57	150	0.52	270	0.52	280	0.61
		[c]	1.63×0.50=	0.82	170	0.93	290	0.93	150	0.95
		[d]	1.63×1.00=	1.63	320	1.28	260	1.13	300	1.13
10	Landers	[a]	1.60×0.30=	0.48	110,120	0.22	220	0.22	270	0.22
		[b]	1.60×0.50=	0.80	300	0.59	70	0.60	110	0.57
		[c]	1.60×0.70=	1.12	140	0.88	240	0.83	100	0.85
		[d]	1.60×1.00=	1.60	140	1.18	260	1.18	300	1.16
11	Landers	[a]	3.34×0.25=	0.84	30,40	0.04	80,90	0.04	120,130	0.04
		[b]	3.34×0.30=	1.00	40	0.65	80	0.66	130	0.65
		[c]	3.34×0.50=	1.67	130	0.95	200	0.91	270	0.94
		[d]	3.34×1.00=	3.34	220	1.29	260	1.42	340	1.29
12	Imperial Valley	[a]	2.82×0.40=	1.13	120	0.09	80	0.09	280	0.10
		[b]	2.82×0.70=	1.97	270	0.47	230	0.61	110	0.52
		[c]	2.82×1.00=	2.82	320	0.82	80	0.87	140	0.90
		[d]	2.82×1.00=	2.82	320	0.82	80	0.87	140	0.90
13	Imperial Valley	[a]	2.04×0.25=	0.51	310	0.17	340	0.17	20	0.17
		[b]	2.04×0.50=	1.02	150	0.54	160	0.52	220	0.54
		[c]	2.04×0.70=	1.43	310	0.73	350	0.71	30	0.72
		[d]	2.04×1.00=	2.04	270	0.95	280	0.97	160	0.96
14	Loma Prieta	[a]	2.23×0.30=	0.67	280	0.20	100	0.21	150	0.20
		[b]	2.23×0.50=	1.12	290	0.58	110	0.57	340	0.58
		[c]	2.23×0.70=	1.56	120	0.93	290	0.92	150	0.91
		[d]	2.23×1.00=	2.23	280	1.17	110	1.16	160	1.13
15	Imperial Valley	[a]	1.69×0.45=	0.76	60	0.19	220	0.18	270	0.21
		[b]	1.69×0.70=	1.18	60	0.39	220	0.37	110	0.57
		[c]	1.69×1.00=	1.69	80	0.93	70	0.77	280	0.98
		[d]	1.69×1.00=	1.69	80	0.93	70	0.77	280	0.98
16	Landers	[a]	4.08×0.30=	1.22	10	0.05	140	0.05	180	0.05
		[b]	4.08×0.50=	2.04	20	0.31	150	0.32	190	0.31
		[c]	4.08×0.70=	2.86	0	0.81	310	0.82	180	0.91
		[d]	4.08×1.00=	4.08	190	1.30	130	1.40	230	1.23
17	N Palm Springs	[a]	4.97×0.30=	1.49	210	0.14	260,270	0.14	310	0.14
		[b]	4.97×0.50=	2.49	200,210	0.49	260	0.49	300	0.50
		[c]	4.97×0.70=	3.48	350	0.74	240	0.75	280	0.84
		[d]	4.97×1.00=	4.97	350	1.07	40	1.03	280	1.05
18	Northridge	[a]	1.56×0.40=	0.62	210	0.16	330	0.17	20	0.17
		[b]	1.56×0.70=	1.09	40	0.60	160	0.60	210	0.59
		[c]	1.56×0.90=	1.40	220	0.89	340	0.87	210	0.85
		[d]	1.56×1.00=	1.56	230	0.91	350	0.93	20	0.92

Table 3 Continued

19	Landers	[a]	$2.74 \times 0.35 =$	0.96	340	0.11	130	0.11	180	0.11
		[b]	$2.74 \times 0.45 =$	1.23	10	0.69	90	0.65	140	0.64
		[c]	$2.74 \times 0.50 =$	1.37	350	0.80	190	1.01	60	0.79
		[d]	$2.74 \times 1.00 =$	2.74	80	1.02	230	1.35	290	1.33
20	Coyote Lake	[a]	$2.70 \times 0.30 =$	0.81	160	0.20	290	0.20	330	0.20
		[b]	$2.70 \times 0.50 =$	1.35	340	0.56	300	0.57	170	0.56
		[c]	$2.70 \times 0.70 =$	1.89	0	0.77	130	0.74	0	0.77
		[d]	$2.70 \times 1.00 =$	2.70	330	0.95	120	0.91	160	0.92

¹: $M_{max}OSDIA$.

²: the biggest scale factor among the ones computed for the three individual pairs.

³: an appropriate factor so that four different intensity levels are achieved.

⁴: minor damage, ⁵: moderate damage, ⁶: severe damage, ⁷: real seismic intensity

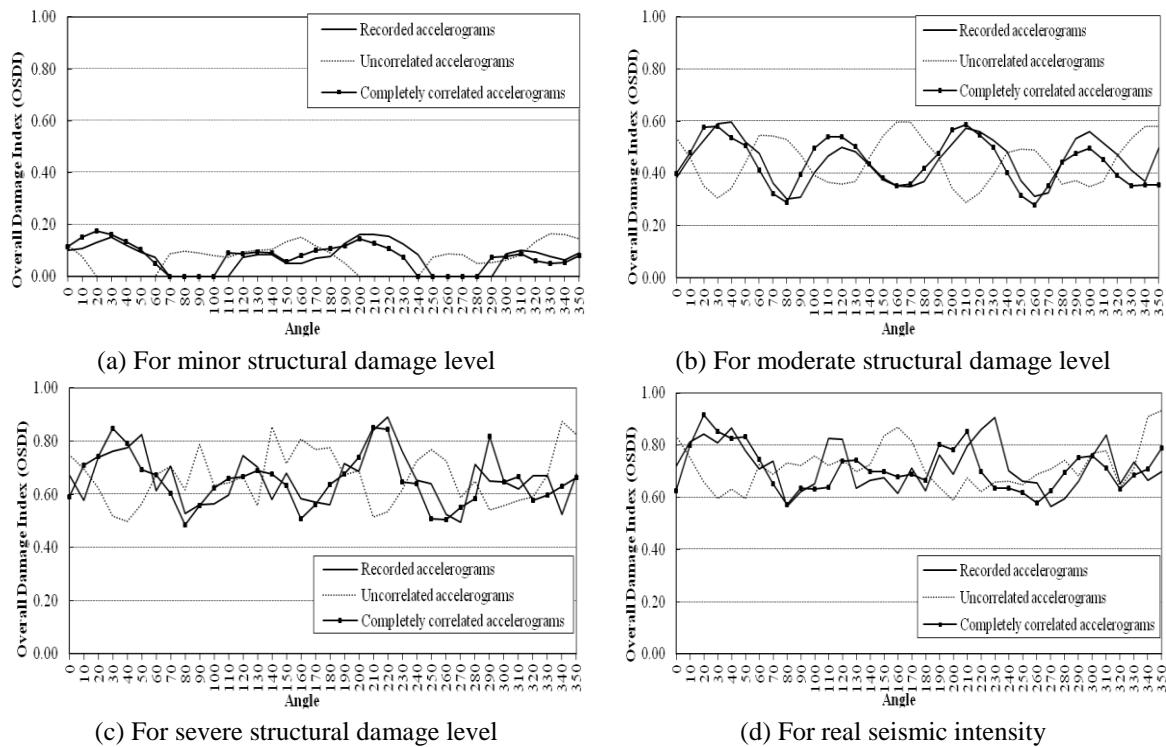


Fig. 5 The overall damage index vs seismic incident angles due to three individual pairs of Northridge - No. 18 ground motion, scaled with the same factor

5. Results

5.1 The three individual pairs of accelerograms are scaled with the same factor

Table 3 presents the $M_{max}OSDIA$ for the four levels of inelastic response caused by the recorded, the uncorrelated and the completely correlated pairs corresponding to the twenty ground

Table 4 MmaxOSDIA for four seismic intensity levels. The three pairs of accelerograms are scaled by different factors

No	Ground motion	Accelerograms											
		Recorded				Uncorrelated				Completely correlated			
		$sf_{scaling,rec}^2 \times sf_{int.level}^5 = SF_{rec}$	Angle (deg)	D^1		$sf_{scaling,un}^3 \times sf_{int.level} = SF_{un}$	Angle(deg)	D^1		$sf_{scaling,cor}^4 \times sf_{int.level} = SF_{co}$	Angle (deg)	D^1	
1	Northridge	[a]	1.56×0.42= 0.66	30,40	0.08	[a]	1.57×0.42= 0.66	210	0.07	[a]	1.54×0.42= 0.65	260	0.07
		[b]	1.56×0.55= 0.86	250	0.63	[b]	1.57×0.55= 0.86	230	0.70	[b]	1.54×0.55= 0.85	110	0.61
		[c]	1.56×0.70= 1.09	50	0.89	[c]	1.57×0.70= 1.10	70	0.95	[c]	1.54×0.70= 1.08	290	0.78
		[d]	1.56×1.00= 1.56	170	1.09	[d]	1.57×1.00= 1.57	50	1.06	[d]	1.54×1.00= 1.54	110	1.04
2	Northridge	[a]	1.38×0.20= 0.28	160	0.05	[a]	1.25×0.20= 0.25	-	0.00	[a]	1.35×0.20= 0.27	300-320	0.04
		[b]	1.38×0.30= 0.41	140	0.59	[b]	1.25×0.30= 0.38	60	0.63	[b]	1.35×0.30= 0.41	290	0.59
		[c]	1.38×0.50= 0.69	230	1.00	[c]	1.25×0.50= 0.63	250	1.00	[c]	1.35×0.50= 0.68	20	0.90
		[d]	1.38×1.00= 1.38	200	1.17	[d]	1.25×1.00= 1.25	210	1.10	[d]	1.35×1.00= 1.35	320	1.15
3	Loma Prieta	[a]	1.00×0.40= 0.40	330	0.15	[a]	1.00×0.40= 0.40	330	0.15	[a]	1.01×0.40= 0.40	20	0.16
		[b]	1.00×1.00= 1.00	330	0.68	[b]	1.00×1.00= 1.00	160	0.67	[b]	1.01×1.00= 1.01	20	0.68
		[c]	1.00×1.40= 1.40	250	0.87	[c]	1.00×1.40= 1.40	340	0.85	[c]	1.01×1.40= 1.41	30	0.86
		[d]	1.00×1.00= 1.00	330	0.68	[d]	1.00×1.00= 1.00	160	0.67	[d]	1.01×1.00= 1.01	20	0.68
4	Loma Prieta	[a]	2.96×0.30= 0.89	260	0.12	[a]	3.08×0.30= 0.92	70	0.13	[a]	2.92×0.30= 0.88	120	0.11
		[b]	2.96×0.70= 2.07	90	0.61	[b]	3.08×0.70= 2.16	90	0.64	[b]	2.92×0.70= 2.04	310	0.61
		[c]	2.96×1.00= 2.96	270	0.88	[c]	3.08×1.00= 3.08	90	0.88	[c]	2.92×1.00= 2.92	130	0.88
		[d]	2.96×1.00= 2.96	270	0.88	[d]	3.08×1.00= 3.08	90	0.88	[d]	2.92×1.00= 2.92	130	0.88
5	Whittier Narrows	[a]	2.60×0.40= 1.04	260	0.13	[a]	2.46×0.40= 0.98	280, 290	0.10	[a]	2.58×0.40= 1.03	330	0.13
		[b]	2.60×0.90= 2.34	80	0.70	[b]	2.46×0.90= 2.21	110	0.60	[b]	2.58×0.90= 2.32	150	0.65
		[c]	2.60×1.10= 2.86	240	0.80	[c]	2.46×1.10= 2.71	100	0.78	[c]	2.58×1.10= 2.84	330	0.79
		[d]	2.60×1.00= 2.60	250	0.75	[d]	2.46×1.00= 2.46	120	0.75	[d]	2.58×1.00= 2.58	140	0.75
6	Imperial Valley	[a]	3.58×0.30= 1.07	80	0.13	[a]	3.91×0.30= 1.17	240	0.22	[a]	3.54×0.30= 1.06	280, 290	0.16
		[b]	3.58×0.60= 2.15	130	0.62	[b]	3.91×0.60= 2.35	70	0.68	[b]	3.54×0.60= 2.12	120	0.62
		[c]	3.58×0.85= 3.04	320	0.81	[c]	3.91×0.85= 3.32	240	0.87	[c]	3.54×0.85= 3.01	290	0.78
		[d]	3.58×1.00= 3.58	200	0.98	[d]	3.91×1.00= 3.91	250	1.05	[d]	3.54×1.00= 3.54	300	0.96
7	San Fernando	[a]	2.88×0.30= 0.86	-	0.00	[a]	3.88×0.30= 1.16	280	0.25	[a]	2.84×0.30= 0.85	-	0.00
		[b]	2.88×0.50= 1.44	70	0.34	[b]	3.88×0.50= 1.94	290	0.59	[b]	2.84×0.50= 1.42	70	0.60
		[c]	2.88×0.70= 2.02	270	0.64	[c]	3.88×0.70= 2.72	290	0.79	[c]	2.84×0.70= 1.99	320	0.82
		[d]	2.88×1.00= 2.88	250	0.86	[d]	3.88×1.00= 3.88	80	1.20	[d]	2.84×1.00= 2.84	310	0.92

Table 4 Continued

8	Loma Prieta	[a]	1.94×0.50=	0.97	40	0.19	[a]	2.06×0.50=	1.03	180, 190	0.20	[a]	1.94×0.50=	0.97	220	0.19
		[b]	1.94×0.70=	1.36	60	0.38	[b]	2.06×0.70=	1.44	190	0.43	[b]	1.94×0.70=	1.36	230	0.38
		[c]	1.94×1.00=	1.94	50	0.68	[c]	2.06×1.00=	2.06	350	0.77	[c]	1.94×1.00=	1.94	230	0.70
		[d]	1.94×1.00=	1.94	50	0.68	[d]	2.06×1.00=	2.06	350	0.77	[d]	1.94×1.00=	1.94	230	0.70
9	Northridge	[a]	1.54×0.30=	0.46	330	0.05	[a]	1.63×0.30=	0.49	260	0.11	[a]	1.60×0.30=	0.48	120	0.08
		[b]	1.54×0.35=	0.54	320	0.44	[b]	1.63×0.35=	0.57	270	0.52	[b]	1.60×0.35=	0.56	130	0.47
		[c]	1.54×0.50=	0.77	340	0.86	[c]	1.63×0.50=	0.82	290	0.93	[c]	1.60×0.50=	0.80	250	0.77
		[d]	1.54×1.00=	1.54	130	1.27	[d]	1.63×1.00=	1.63	260	1.13	[d]	1.60×1.00=	1.60	110	1.12
10	Landers	[a]	1.59×0.30=	0.48	110	0.22	[a]	1.60×0.30=	0.48	220	0.22	[a]	1.57×0.30=	0.47	270	0.21
		[b]	1.59×0.50=	0.80	310	0.56	[b]	1.60×0.50=	0.80	70	0.60	[b]	1.57×0.50=	0.79	110	0.56
		[c]	1.59×0.70=	1.11	310	0.85	[c]	1.60×0.70=	1.12	240	0.83	[c]	1.57×0.70=	1.10	100	0.83
		[d]	1.59×1.00=	1.59	140	1.15	[d]	1.60×1.00=	1.60	260	1.18	[d]	1.57×1.00=	1.57	130	1.14
11	Landers	[a]	3.33×0.25=	0.83	30	0.04	[a]	2.98×0.25=	0.75	-	0.00	[a]	3.34×0.25=	0.84	120, 130	0.04
		[b]	3.33×0.30=	1.00	40	0.65	[b]	2.98×0.30=	0.89	260	0.08	[b]	3.34×0.30=	1.00	130	0.65
		[c]	3.33×0.50=	1.67	150	0.91	[c]	2.98×0.50=	1.49	260	0.88	[c]	3.34×0.50=	1.67	270	0.94
		[d]	3.33×1.00=	3.33	220	1.29	[d]	2.98×1.00=	2.98	300	1.38	[d]	3.34×1.00=	3.34	340	1.29
12	Imperial Valley	[a]	2.81×0.40=	1.12	120	0.09	[a]	2.67×0.40=	1.07	90	0.07	[a]	2.82×0.40=	1.13	280	0.10
		[b]	2.81×0.70=	1.97	310	0.47	[b]	2.67×0.70=	1.87	300	0.40	[b]	2.82×0.70=	1.97	110	0.52
		[c]	2.81×1.00=	2.81	320	0.80	[c]	2.67×1.00=	2.14	70	0.93	[c]	2.82×1.00=	2.26	140	0.90
		[d]	2.81×1.00=	2.81	320	0.80	[d]	2.67×1.00=	2.67	70	0.93	[d]	2.82×1.00=	2.82	140	0.90
13	Imperial Valley	[a]	1.90×0.25=	0.48	310	0.13	[a]	1.91×0.25=	0.48	330	0.13	[a]	2.04×0.25=	0.51	20	0.17
		[b]	1.90×0.50=	0.95	140	0.50	[b]	1.91×0.50=	0.96	160	0.50	[b]	2.04×0.50=	1.02	220	0.54
		[c]	1.90×0.70=	1.33	140	0.70	[c]	1.91×0.70=	1.34	170	0.71	[c]	2.04×0.70=	1.43	30	0.72
		[d]	1.90×1.00=	1.90	300	0.89	[d]	1.91×1.00=	1.91	270	0.93	[d]	2.04×1.00=	2.04	160	0.96
14	Loma Prieta	[a]	2.22×0.30=	0.67	280,290	0.20	[a]	2.23×0.30=	0.67	100	0.21	[a]	2.12×0.30=	0.64	150	0.18
		[b]	2.22×0.50=	1.11	290	0.58	[b]	2.23×0.50=	1.12	110	0.57	[b]	2.12×0.50=	1.06	150, 160	0.53
		[c]	2.22×0.70=	1.55	120	0.93	[c]	2.23×0.70=	1.56	290	0.92	[c]	2.12×0.70=	1.48	330	0.86
		[d]	2.22×1.00=	2.22	290	1.17	[d]	2.23×1.00=	2.23	110	1.16	[d]	2.12×1.00=	2.12	150	1.10
15	Imperial Valley	[a]	1.69×0.45=	0.76	60	0.19	[a]	1.59×0.45=	0.72	230	0.13	[a]	1.67×0.45=	0.75	270	0.19
		[b]	1.69×0.70=	1.18	60	0.39	[b]	1.59×0.70=	1.11	40	0.35	[b]	1.67×0.70=	1.17	90	0.38
		[c]	1.69×1.00=	1.69	80	0.93	[c]	1.59×1.00=	1.59	70	0.71	[c]	1.67×1.00=	1.67	120	0.87
		[d]	1.69×1.00=	1.69	80	0.93	[d]	1.59×1.00=	1.59	70	0.71	[d]	1.67×1.00=	1.67	120	0.87

Table 4 Continued

16	Landers	[a]	3.53×0.30=	1.06	-	0.00	[a]	4.08×0.30=	1.22	140	0.05	[a]	3.55×0.30=	1.07	-	0.00
		[b]	3.53×0.50=	1.77	0	0.23	[b]	4.08×0.50=	2.04	150	0.32	[b]	3.55×0.50=	1.78	180	0.23
		[c]	3.53×0.70=	2.47	30	0.45	[c]	4.08×0.70=	2.86	310	0.82	[c]	3.55×0.70=	2.49	200	0.45
		[d]	3.53×1.00=	3.53	90	1.09	[d]	4.08×1.00=	4.08	130	1.40	[d]	3.55×1.00=	3.55	60	1.16
17	N Palm Springs	[a]	4.72×0.30=	1.42	210	0.12	[a]	4.97×0.30=	2.39	260, 270	0.14	[a]	4.56×0.30=	1.37	310	0.10
		[b]	4.72×0.50=	2.36	210	0.47	[b]	4.97×0.50=	3.99	260	0.49	[b]	4.56×0.50=	2.28	310	0.43
		[c]	4.72×0.70=	3.30	350	0.69	[c]	4.97×0.70=	5.58	240	0.75	[c]	4.56×0.70=	3.19	280	0.78
		[d]	4.72×1.00=	4.72	170	0.98	[d]	4.97×1.00=	7.97	40	1.03	[d]	4.56×1.00=	4.56	80	1.02
18	Northridge	[a]	1.38×0.40=	0.55	210	0.10	[a]	1.56×0.40=	0.62	330	0.17	[a]	1.40×0.40=	0.56	20	0.10
		[b]	1.38×0.70=	0.97	220	0.46	[b]	1.56×0.70=	1.09	160	0.6	[b]	1.40×0.70=	0.98	30	0.48
		[c]	1.38×0.90=	1.24	320	0.72	[c]	1.56×0.90=	1.40	340	0.87	[c]	1.40×0.90=	1.26	210	0.72
		[d]	1.38×1.00=	1.38	220	0.84	[d]	1.56×1.00=	1.56	350	0.93	[d]	1.40×1.00=	1.40	30	0.90
19	Landers	[a]	2.74×0.35=	0.96	340	0.11	[a]	2.59×0.35=	0.91	130	0.07	[a]	2.48×0.35=	0.87	170	0.06
		[b]	2.74×0.45=	1.23	10	0.69	[b]	2.59×0.45=	1.17	130	0.51	[b]	2.48×0.45=	1.12	200	0.26
		[c]	2.74×0.50=	1.37	350	0.80	[c]	2.59×0.50=	1.30	160	0.91	[c]	2.48×0.50=	1.24	140	0.65
		[d]	2.74×1.00=	2.74	80	1.02	[d]	2.59×1.00=	2.59	70	1.33	[d]	2.48×1.00=	2.48	20	1.20
20	Coyote Lake	[a]	2.36×0.30=	0.71	150,160	0.12	[a]	2.70×0.30=	0.81	290	0.20	[a]	2.35×0.30=	0.71	340	0.12
		[b]	2.36×0.50=	1.18	170	0.45	[b]	2.70×0.50=	1.35	300	0.57	[b]	2.35×0.50=	1.18	350	0.45
		[c]	2.36×0.70=	1.65	160	0.71	[c]	2.70×0.70=	1.89	130	0.74	[c]	2.35×0.70=	1.65	160	0.74
		[d]	2.36×1.00=	2.36	170	0.92	[d]	2.70×1.00=	2.70	120	0.91	[d]	2.35×1.00=	2.35	170	0.92

¹: M_{\max} OSDIA.

²: Scale factor computed by the scaling procedure of the recorded accelerograms

³: Scale factor computed by the scaling procedure of the uncorrelated accelerograms

⁴: Scale factor computed by the scaling procedure of the completely correlated accelerograms

⁵: the same factor used in Table 3 for each ground motion and intensity level.

motions under consideration scaled with the same factor, sf_{scaling} , produced by the scaling procedure. Figs. 5(a), (b), (c) and (d) show the plot of the OSDI vs incident angle under the three pairs of Northridge – No. 18 ground motion for the four levels of inelastic response. As mentioned above, in order to get the four levels of inelastic response the three pairs of accelerograms are multiplied by an appropriate factor sf_{scaling} (e.g., for the Northridge – No. 18 ground motion the values of the factor sf_{scaling} are 0.40, 0.70, 0.90 and 1.00 for minor damage, moderate damage, severe damage and real seismic intensity respectively (Table 3)).

We see that for the most of the examined ground motions the recorded, the uncorrelated as well as the completely correlated pairs of accelerograms exhibit approximately the same extent of damage for the critical angle of seismic incidence (i.e. the angle that yields the maximum value of OSDI). For example, the values of $M_{\text{max}}\text{OSDIA}$ for Northridge – No. 18 ground motion for the four intensity levels, are 0.16, 0.60, 0.89 and 0.91 due to recorded, 0.17, 0.60, 0.87 and 0.93 due to uncorrelated and 0.17, 0.59, 0.85 and 0.92 due to completely correlated pair of accelerograms (Table 3). An exception to this is the Imperial Valley-No12 ground motion that produces values of $M_{\text{max}}\text{OSDIA}$ equal to 0.47 (recorded accelerograms), 0.61 (uncorrelated accelerograms) and 0.52 (completely correlated accelerograms) for moderate damage level; the Imperial Valley-No 15 that produces values equal to 0.39 (recorded accelerograms), 0.37 (uncorrelated accelerograms) and 0.57 (completely correlated accelerograms) for moderate damage level and the Landers-No 19 that produces values equal to 0.80 (recorded accelerograms), 1.01 (uncorrelated accelerograms) and 0.79 (completely correlated accelerograms) for severe damage level.

5.2 The three individual pairs of accelerograms are scaled with different factor

Table 4 presents the $M_{\text{max}}\text{OSDIA}$ produced by the recorded, the uncorrelated and the completely correlated pairs of accelerograms corresponding to the twenty ground motions under consideration. The accelerograms are scaled with different factors. In particular, the three pairs of accelerograms are multiplied by the scale factor, sf_{scaling} , produced by the ASCE 41-06 procedure. As mentioned above, the scale factor is different for each individual pair of accelerograms (recorded, uncorrelated and completely correlated). For example under Northridge – No 18 ground motion the scale factors are 1.38, 1.56 and 1.40 for the recorded, the uncorrelated and the completely correlated accelerograms respectively. Furthermore the three pairs of accelerograms are multiplied by an appropriate factor ($sf_{\text{intensity level}}$) corresponding to each ground motion and intensity level. This factor is equal to the one used in the previous section so that the two examined cases (5.1 and 5.2) are comparable.

Figs. 6(a), (b), (c) and (d) present the plot of OSDI vs incident angle caused by the three individual pairs of accelerograms under – No. 18 ground motion. The accelerograms are scaled with different scale factor, that is the one produced by the scaling procedure for each individual pair. As can be seen in Figs. 6(a), (b), (c) and (d) and in Table 4, the $M_{\text{max}}\text{OSDIA}$ produced by the recorded, the uncorrelated and the completely correlated accelerograms is different. For example, for damage level [d] the $M_{\text{max}}\text{OSDIA}$ is 0.84, 0.93 and 0.90 for the recorded, the uncorrelated and the completely correlated pairs of accelerograms corresponding to Northridge No. 18 ground motion, respectively (Fig. 6(d) and Table 4). Also note that the three pairs of accelerograms can cause different extent of structural damage when they are scaled with different scale factor (records No. 5, 7, 8, 11 and 16). See for example No. 11 ground motion (Table 4) for damage level [b]. The $M_{\text{max}}\text{OSDIA}$ is 0.65, 0.08 and 0.65 due to the recorded, the uncorrelated and the completely correlated accelerograms respectively. We should note that for the same ground motion

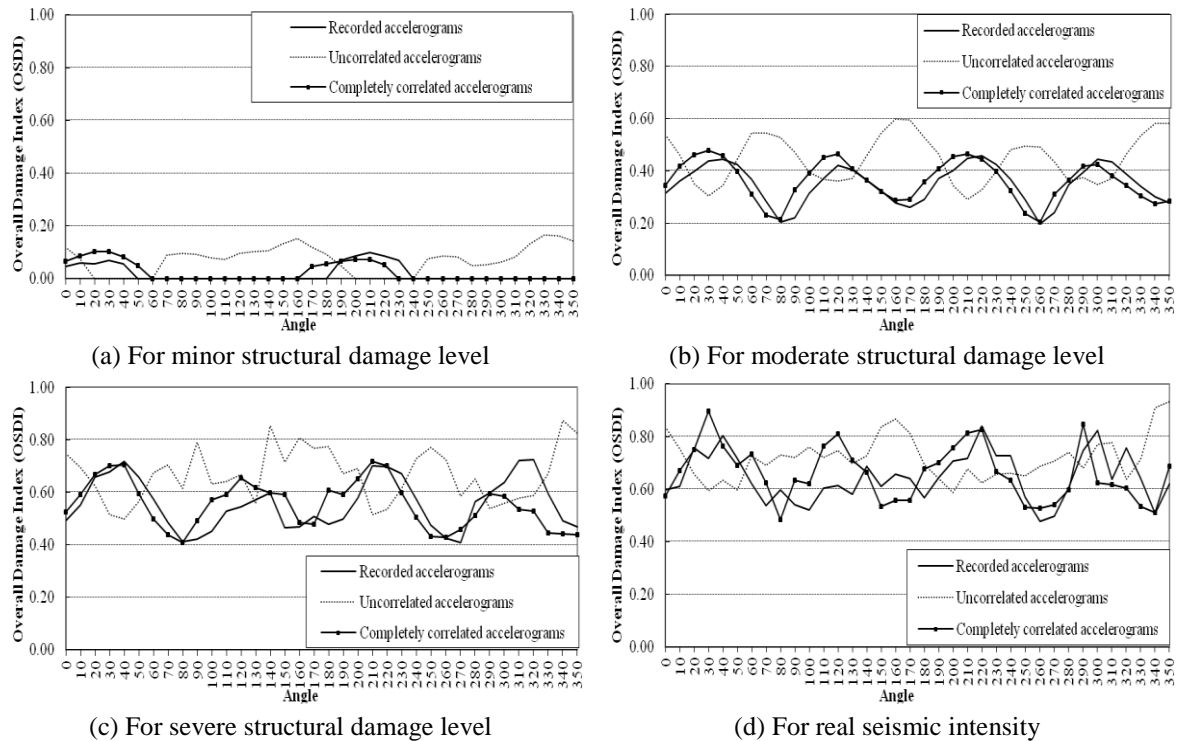


Fig. 6 The overall damage index vs seismic incident angles due to three individual pairs of Northridge – No. 18 ground motion scaled with different scale factor

and damage level, the three pairs of accelerograms produce quite the same value of M_{\max} OSDIA when they are scaled with the same factor each (Table 3).

5.3 General results

The damage index depends strongly on (a) the seismic incident angle and (b) the ground-motion reference axes. Focusing on the seismic incident angle, we can see in Fig. 5(c) that for severe damage level the OSDI due to Northridge - No. 18 ground motion ranges between 0.49-0.90 for the recorded, 0.50-0.87 for the uncorrelated and 0.49-0.85 for the completely correlated pairs of accelerograms. It is worth mentioning that for the majority of the incident angles the three individual pairs of the same ground motion (recorded, uncorrelated and completely correlated) produce different structural damage indices.

Another important observation is that the critical incident angle (i.e., the angle that yields the maximum damage index) does not coincide with the principal axes of the building (incident angles $\theta=0^\circ$ and $\theta=90^\circ$). Results demonstrate that the use of the recorded pairs of accelerograms as seismic input for seismic incident angles 0° and 90° does not always lead to the critical case of study. However, no specific references concerning this subject is given in the code provisions worldwide.

Also note that the critical incident angle is different for various seismic intensity levels (Figs. 5(b), 5(c) and Figs 6(b), 6(c)). Furthermore, observe that for minor structural damage level the plot

of the overall damage index vs seismic incident angle is generally quite smooth (Fig. 5(a) and Fig. 6(a)). On the contrary, the plot of overall damage index vs seismic incident angle becomes jagged (more peaks in smaller range of angles) as the inelastic level increases (Figs. 5(b), 5(c), 5(d), 6(c) and 6(d)).

Moreover, one can see that the critical incident angle large depends on the pair of accelerograms used as seismic input. For instance, for the recorded and the completely correlated pairs of accelerograms (Northridge – No. 18) and for moderate seismic intensity level the angle that causes maximum OSDI is 40° and 210° respectively (Fig. 5(b) and Table 3). However, this orientation causes little damage (OSDI=0.30) under the uncorrelated accelerograms.

Next, investigating the effect of the orientation of ground-motion reference axes (recorded, uncorrelated and completely correlated accelerograms) on the M_{\max} OSDIA we see (Table 3) that under No. 12 ground motion, for moderate damage level the values of M_{\max} OSDIA are 0.47, 0.61 and 0.52 under the recorded, the uncorrelated and the completely correlated accelerograms, respectively. Also see No. 9 (moderate damage level), No. 15 (moderate and severe damage level) as well as No. 19 (severe damage level).

Moreover, one can see (Table 3) that under No. 18 ground motion, for severe damage level the recorded accelerograms cause maximum value of M_{\max} OSDIA, while under No. 20 ground motion the recorded and the completely correlated accelerograms cause maximum value of M_{\max} OSDIA. Also, one can see that under No. 5 ground motion for moderate damage level the completely correlated accelerograms cause M_{\max} OSDIA while for severe damage level the uncorrelated accelerograms cause M_{\max} OSDIA. The results due to all ground motions considered in the present study show that any of the three individual pairs of accelerograms has the potential to maximize the damage index. This is true not only for different ground motions but also for different intensity levels of the same ground motion. The above observations are valid for all ground motions considered in the present study.

6. Conclusions

The influence of some parameters on the overall damage index of an asymmetric single storey r/c building is investigated. The key parameters are: i) seismic incident angle, ii) ground-motion reference axes and iii) seismic intensity level. Nonlinear dynamic analyses under twenty bi-directional ground motions for many seismic incident angles, for four intensity levels are performed and the overall damage index is computed.

From the scaling procedure the following conclusions can be drawn:

- The SRSS spectra obtained by the two horizontal components of the recorded, the uncorrelated and the completely correlated accelerograms corresponding to the same ground motion are different. As a consequence the scale factors produced by the recorded, the uncorrelated and the completely correlated pairs of accelerograms corresponding to the same ground motion are different.

- The EC8 scaling procedure is more conservative (for the ground motions considered) providing scale factors up to 2.2 times larger than the corresponding scale factors computed by ASCE 41-06 procedure.

From the nonlinear dynamic analyses the following conclusions can be drawn.

Considering the effect of seismic incident angle:

- The variability of structural response to the direction of seismic input becomes larger as the

level of inelastic behaviour increases. For minor structural damage level the plot of the overall damage index vs seismic incident angle is generally smooth. However, the plot of the overall damage index vs seismic incident angle becomes jagged as the inelastic level increases.

- There is not a particular seismic incident angle or range of angles that leads to the maximum values of damage index regardless of the seismic intensity level or the ground-motion reference axes.

Considering the effect of ground-motion reference axes:

- For the examined cases the maximum value of the damage index does not occur when the accelerograms act along the structural axes.

- The three individual pairs of accelerograms corresponding to the same ground motion (recorded, uncorrelated and completely correlated) can cause different values of the structural damage index for the same incident angle.

- The three individual pairs of accelerograms multiplied by the same scale factor cause approximately the same extend of structural damage for the critical angle of seismic incidence.

- The three individual pairs of accelerograms corresponding to the same ground motion scaled according to ASCE 41-06 procedure (with different scale factor each pair) can cause different level of structural damage for the critical angle of seismic incidence.

- Any individual pair of accelerograms (recorded, uncorrelated and completely correlated) has the potential to cause the maximum value of the damage index. This is true not only for different ground motions but also for different seismic intensity levels of the same ground motion.

The above results demonstrate that nonlinear structural response is affected by the seismic incident angle, the ground-motion reference axes (recorded, uncorrelated and completely correlated accelerograms) as well as the seismic intensity level. Nevertheless, in order to draw general and conclusive results concerning the herein investigated issues further detailed investigation is needed.

References

- Arias, A. (1970), "A measure of earthquake intensity", Ed. Hansen, R.J., *Seismic Design for Nuclear Power Plants*, The MIT Press, Cambridge, MA.
- Athanatopoulou, A.M. (2005), "Critical orientation of three correlated seismic components", *Eng. Struct.*, **27**, 301-12.
- Athanatopoulou, A.M. and Avramidis, I.E. (2006), "Effects of seismic directivity on structural response", *Proceedings of 2nd fib Congress*, Naples, Italy, Paper ID 8-15.
- Athanatopoulou, A.M., Tsourekas, A. and Papamanolis, G. (2005), "Variation of response with incident angle under two horizontal correlated seismic components", *Proceedings of the Earthquake Resistant Engineering Structure V*, Skiathos, Greece.
- Athanatopoulou, A.M., Anastasiadis, K. and Avramidis, I.E. (2006), "Influence of seismic incident angle on response values", *Proceedings of 15th Greek Conference of Concrete Structures*, Vol. B, Alexandroupoli, Greece. (in Greek)
- ASCE 41-06 (2009), *Seismic Rehabilitation of Existing Buildings*, American Society of Civil Engineers, Reston, Virginia.
- Beyer, K. and Bommer, J. (2007), "Selection and scaling of real accelerograms for bi-directional loading: a review of current practice and code provisions", *J. Earthq. Eng.*, **11**, 13-45.
- Catalan, A., Benavent-Climent, A. and Cahisc, X. (2010), "Selection and scaling of earthquake records in assessment of structures in low-to-moderate seismicity zones", *Soil Dyn. Earthq. Eng.*, **30**(1-2), 40-49.
- Carr, A.J. (2004), "Ruaumoko - a program for inelastic time-history analysis, Program manual", Department

- of Civil Engineering, University of Canterbury, New Zealand
- CEN (2003), Eurocode 8, Design of structures for earthquake resistance, Part 1: General rules, seismic actions and rules for buildings, European Committee for Standardization, Brussels.
- Chen, C. (1975), "Definition of Statistically Independent Time Histories", *J. Struct. Div.*, ASCE, **101**(Nst2), 449-451.
- Dolsek, M. and Fajfar, P. (2002), "Mathematical modeling of an infilled RC frame structure based on the results of pseudo-dynamic tests", *Earthq. Eng. Struct. Dyn.*, **31**, 1215-1230.
- EAK 2003 (2003), *Greek Code for Earthquake Resistant Design of Structures*, Ministry of Environment, Planning and Public Works, Greece
- EKOS 2000 (2000), *Greek Code for the Design and Construction of Concrete Works*, Greek Ministry of Environment, Planning and Public Works, Greece
- Hancock, J. and Bommer, J.J. (2008), "Numbers of scaled and matched accelerograms required for inelastic dynamic analyses", *Earthq. Eng. Struct. Dyn.*, **37**(14), 1585-1607.
- Kostinakis, K., Athanatopoulou, A. and Avramidis, I. (2008), "Maximum response and critical incident angle in special classes of buildings subjected to two horizontal seismic components", *Proceedings of the 6th GRACM International Congress on Computational Mechanics*, Thessaloniki, Greece.
- Khoshnoudian, F. and Poursha, M. (2004), "Response of three dimensional buildings under bi-directional and unidirectional seismic excitations", *Proceedings of 13th world conference on earthquake engineering*.
- Lagaros, N.D. (2010a), "Multicomponent incremental dynamic analysis considering variable incident angle", *Struct. Infrastr. Eng.*, **6**, 77-94.
- Lagaros, N.D. (2010b), "The impact of the earthquake incident angle on the seismic loss estimation", *Eng. Struct.*, **32**, 1577-1589.
- Nguyen, V.T. and Kim, D.K. (2013), "Influence of incident angles of earthquakes on inelastic responses of asymmetric-plan structures", *Struct. Eng. Mech.*, **45**(3), 373-389.
- Lucchini, A., Monti, G. and Kunnath, S. (2011), "Nonlinear response of two-way asymmetric single-story building under biaxial excitation", *J. Struct. Eng.*, **137**(1), 34-40.
- MacRae, G.A. and Mattheis, J. (2000), "Three dimensional steel building response to near-fault motions", *J. Struct. Eng.*, ASCE, **126**(1), 117-26.
- Oyarzo-Vera, C. and Chouw, N. (2008), "Comparison of record scaling methods proposed by standards currently applied indifferent countries", *Proceedings of 14th World Conference on Earthquake Engineering*, Beijing, China.
- FEMA 356 (2000), Prestandard and commentary for the seismic rehabilitation of buildings, Federal Emergency Management Agency, Washington, D.C.
- Park, Y.J. and Ang, A.H.S. (1985), "Mechanistic seismic damage model for reinforced concrete", *J. Struct. Eng.*, ASCE, **111**(ST4), 722-739.
- Pacific Earthquake Engineering Research Center (PEER) (2003), Strong Motion Database, <http://peer.berkeley.edu/smcat>. PEER (2005), NGA database (where NGA stands for "Next Generation of Attenuation") with records orientated in fault-normal and fault-parallel orientation, PEER strong-motion database (<http://peer.berkeley.edu/nga/index.html>), Pacific Earthquake Engineering Research Center, Berkeley.
- Penzien, J. and Watabe, M. (1975), "Characteristics of 3-D earthquake ground motions", *Earthq. Eng. Struct. Dyn.*, **3**, 365-373.
- Reyes, J.C. and Chopra, A.K. (2012), "Modal pushover-based scaling of two components of ground motion records for nonlinear RHA of structures", *Earthq. Spectra*, **28**(3), 1243-1267.
- Rigato, A.B. and Medina, R.A. (2007), "Influence of angle of incidence on seismic demands for single-storey structures subjected to bi-directional ground motions", *Eng. Struct.*, **29**, 2593-2601.
- Stathopoulos, K.G. and Anagnostopoulos, S.A. (2005), "Inelastic torsion of multistorey buildings under earthquake excitations", *Earthq. Eng. Struct. Dyn.*, **34**, 1449-1465.
- Takewaki, I. and Tsujimoto, H. (2011), "Scaling of design earthquake ground motions for tall buildings based on drift and input energy demands", *Earthq. Struct.*, **2**(2), 171-187.
- Wood, R.L. and Hutchinson, T.C. (2012), "Effects of ground motion scaling on nonlinear higher mode

- building response”, *Earthq. Struct.*, **3**(6), 869-887.
- Zhang, Y., Li, W.Q. and Fan, J.S. (2011), “Influence of earthquake attack angle on seismic demands for structures under bi-directional ground motions”, *Adv. Mater. Res.*, **255-260**, 2330-2334.
- Zhang, Y., Li, Q.W. and Fan, J.S. (2012), “The maximum structural response of structures under bi-directional earthquake ground motions”, *Gongcheng Lixue/Eng. Mech.*, **29**(11), 129-136.

CC